A simulation model to improve pneumatic intensifier performance and reliability

by C. Scheffer* and A. Basson*

Synopsis

This paper describes a model that can simulate the behaviour of a pneumatic intensifier that is generally referred to as an 'air pump' (AP). The AP is used in many South African underground mines, and utilizes compressed air with pressures between 0.3–0.6 MPa to pump water up to pressures of 12–18 MPa. The high pressure water is used in numerous underground mines to pressurize props and roof bolts that act as safety and roof support devices. The simulation model reproduces the intensifier's operation under various conditions and therefore can be used to investigate the AP's sensitivity towards environmental conditions, design parameters (such as spring stiffness, plunger diameter, nozzle diameter etc.) and operating conditions. Model validation by comparison with laboratory experiments showed good correlation. The model can subsequently be used to investigate design changes aimed at improving the AP's performance and reliability over a wider range of operating conditions.

Introduction

New Concept Mining (Pty) Ltd manufactures a pneumatic intensifier for use in underground mines, called the 'air pump' (AP). It uses compressed air to pump water, and has a pressure ratio of about 33:1. This means that a supply air pressure of 0.4 MPa will result in a water delivery pressure of 13.2 MPa. The regular version of the AP has to deliver at least 12 MPa for use with mining props called Jackpots, which are used to prestress timber poles that supply roof support in underground mines. The AP is also used with various other underground prop and roof bolt type devices, and it is hence a crucial device to ensure safety in underground mines.

The simulation model presented here was developed to investigate the AP's performance characteristics. The model's intended use is to explore the physical phenomena that determine the operational envelope of the current AP and to investigate potential design changes. The model is based on a particular combination of first principles equations, empirical correlations and numerical techniques, which is shown in this paper to reproduce the behaviour of the AP with sufficient accuracy for the previously mentioned objectives. The authors believe that similar combinations of techniques can be applied to advance the development of similar mining equipment.

The basic operation of the AP is as follows (refer to Figure 1): During the delivery stroke, compressed air moves through the poppet valve to exert enough force on the diaphragm to accelerate the actuator plate forward (right-to-left in Figure 1). The actuator plate is directly connected to a plunger, which pumps the water in the cylinder through the water outlet. At the end of the delivery stroke, the flip-flop valve opens and the poppet valve closes (due to the spring-loaded connection to the plunger), resulting in a release of the high pressure air into the atmosphere. The main diaphragm spring then decelerates the actuator plate and plunger, and returns them to the starting position. During this phase the plunger draws water into the cylinder. One-way valves at the water inlet and outlet control the flow direction. Certain aspects of the AP's design are protected by international patents.

The theory incorporated in the simulation model can be separated into three parts, which are discussed in the following sections: the rigid body dynamics aspects, the fluid mechanics aspects, and the time integration aspects. The relevant literature references are included in these discussions. The experimental work used to validate the simulation model and the comparison of computed vs. measured data are presented after the theoretical aspects. The paper concludes with an assessment of the type of information that can be extracted from the simulation model.

* *Design and Mechatronics Division, Department of Mechanical Engineering, University of Stellenbosch, Matieland.*

 SA ISSN 0038–223X/3.00 + 0.00. Paper received Jan. 2005; revised paper received Mar. 2005.

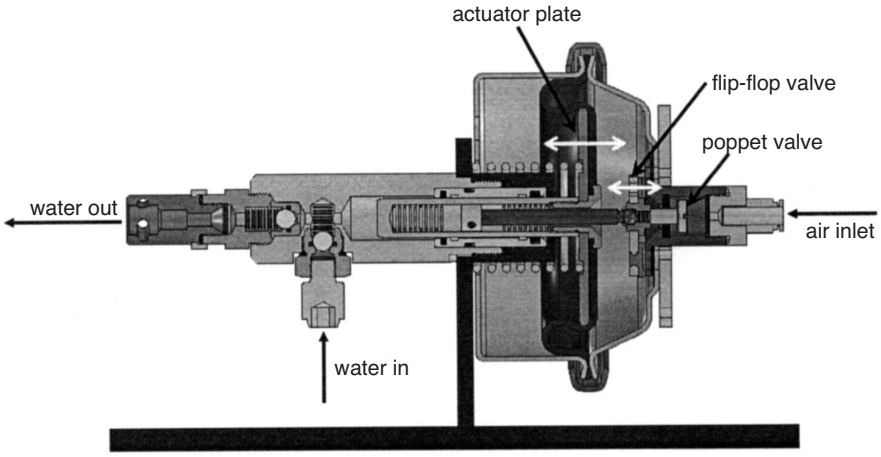

Figure 1—Sectioned drawing of AP main body

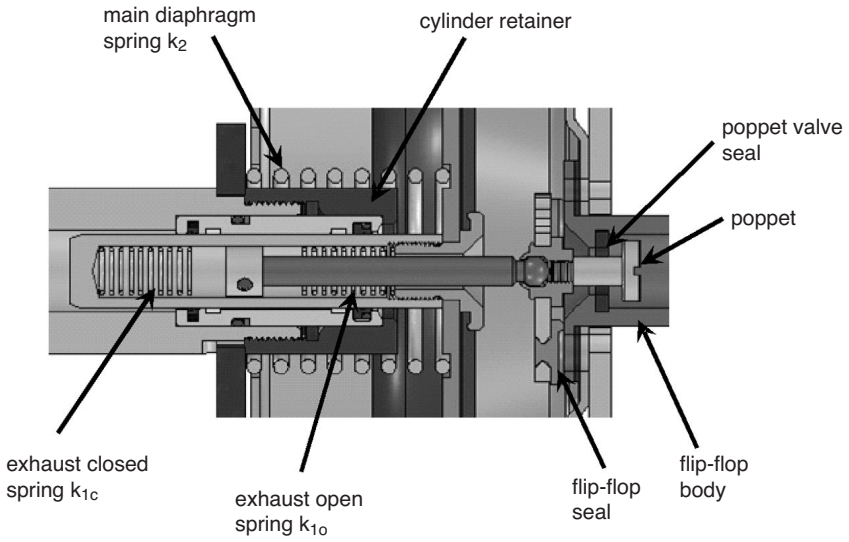

Figure 2—Springs and constraints

Rigid body dynamics

Layout

A sectioned design drawing of the AP is shown in Figure 1. The AP is essentially a two-degree-of-freedom system with motion along one linear axis only. The two assemblies that are moving are the:

- flip-flop valve and parts connected to it, henceforth referred to as m_1
- actuator plate and parts connected to it, henceforth referred to as m_2.

The poppet valve controls the flow of air into the AP, whereas the flip-flop valve essentially controls the flow of air out of the AP. The impacts when these valves open and close are quite extreme, causing high nonlinearities in the model. Furthermore, the maximum and minimum displacement of the actuator and the flip-flop are constrained by the body of the AP itself. Taking a closer look at the AP, in Figure 2, it can be seen that the actuator plate cannot move beyond the cylinder retainer on the forward stroke, or beyond the flip-flop on the return stroke. It can be observed that the displacement of the flip-flip is constrained by the flip-flop body (which is rigidly connected to the actuator housing) and the poppet valve seal. Hence, the maximum travel of the flip-flop is in fact controlled by the length of the poppet's body. Figure 2 also indicates the three springs that control the interaction of the two moving parts in the AP. These are the:

- main diaphragm spring, with spring constant k_2
- exhaust open spring, with spring constant k_{1o}
- exhaust closed spring, with spring constant k_{1c}

Newtonian equations

This section describes the formulation of the Newtonian equations that were used to simulate the AP's operation. The two moving parts that interact with one another, m_1 and m_2, are diagrammatically depicted in Figure 3. The constraints on the system are modelled by means of the rigid ground and a number of discrete springs and dampers between the inertial masses and the ground. These are used to model the impacts when the various constraints in the system become active. The springs are effectively used to stop the displacement in a given direction, whereas the purpose of the dampers is to dissipate the energy associated with the impact.

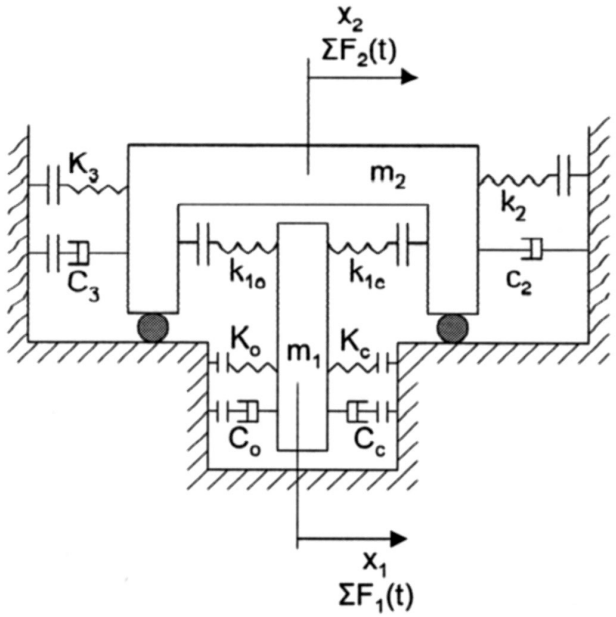

Figure 3—Diagram of AP

The impact spring and dampers are:

- K_o: spring constant when poppet hits seal
- C_o: damping coefficient when poppet hits seal
- K_c: spring constant when flip-flop seal hits flip-flop body
- C_c: damping coefficient when flip-flop seal hits flip-flop body
- K_3: spring constant if actuator plate hits cylinder retainer
- C_3: damping coefficient if actuator plate hits cylinder retainer.

The coefficients listed above are nonlinear functions of x_1 and x_2. Furthermore, some damping was added to the movement of the diaphragm in the form of c_2, to damp the oscillation that is caused by the driving forces. From the diagrams it can also be seen that all the connections between m_1, m_2 and the ground are positively biased (i.e. the springs can only act in compression). The coordinates x_1 and x_2 describe the displacement of m_1 and m_2 in a coordinate system fixed to the ground. The bodies m_1 and m_2 have external forces $\sum F_1(t)$ and $\sum F_2(t)$ acting on them (resulting from the air pressure inside the actuator, and the water pressure acting on the plunger).

Consider the free-body diagram of m_1 depicted in Figure 4. The equation of motion for m_1 can be written as[1]:

$$\begin{aligned} m_1\ddot{x}_1 &= k_{1c}(x_2 - x_1) + K_c(0 - x_1) \\ &+ C_c(0 - \dot{x}_1) - k_{1o}(x_1 - x_2) - K_o(x_1 - o) - C_c \\ (\dot{x}_1 - 0)\textstyle\sum F_1(t) &= -(k_{1o} + k_{1c} + K_o + K_c)x_1 + \\ &(k_{1o} + k_{1c})x_2 - (C_o + C_c)\dot{x}_1 + \textstyle\sum F_1(t) \end{aligned} \quad [1]$$

Consider the free-body diagram of m_2 depicted in Figure 5. The equation of motion for m_2 can be written as[1]:

$$\begin{aligned} m_2\ddot{x}_2 &= k_{1o}(x_1 - x_2) - k_{1c}(x_2 - x_1) - K_3 \\ &(x_2 - 0) - C_3(\dot{x}_2 - 0) + k_2(0 - x_2) + c_2 \\ &(0 - \dot{x}_2) + \textstyle\sum F_2(t) = (k_{1o} + k_{1c})x_1 - \\ &(k_{1o} + k_{1c} + k_2 + K_3)x_2 - (C_3 + c_2)\dot{x}_2 + \textstyle\sum F_2(t) \end{aligned} \quad [2]$$

To enable a numerical solution to Equations [1] and [2], define:

$$\begin{aligned} z_1(t) &= x_1(t) \quad z_3(t) = x_2(t) \\ z_2(t) &= \dot{x}_1(t) \quad z_4(t) = \dot{x}_2(t) \end{aligned} \quad [3]$$

This results in the following useful relationship:

$$\begin{aligned} \dot{z}_1 &= z_2 \\ \dot{z}_3 &= z_4 \end{aligned} \quad [4]$$

Combining [1], [3] and [4]:

$$\dot{z}_2 = -\frac{(k_{1o} + k_{1c} + K_o + K_c)}{m_1} z_1 - \frac{(C_o + C_c)}{m_1} z_2 + \frac{(k_{1o} + k_{1c})}{m_1} z_3 + \frac{\sum F_1(t)}{m_1} \quad [5]$$

Similarly, combining [2],[3] and [4]:

$$\dot{z}_4 = \frac{(k_{1o} + k_{1c})}{m_2} z_1 - \frac{(k_{1o} + k_{1c} + k_2 + K_3)}{m_2} z_3 - \frac{(c_2 + C_3)}{m_2} z_4 + \frac{\sum F_2(t)}{m_2} \quad [6]$$

Equations [5] and [6] can be written in matrix form as:

$$\dot{\underset{\sim}{z}}(t) = A\underset{\sim}{z}(t) + B\underset{\sim}{f}(t) \quad [7]$$

Equation [7] is a first-order differential equation that can be solved with numerical integration. In this case, MATLAB[2] was used for a numerical implementation of the Runga-Kutta method of numerical integration[3].

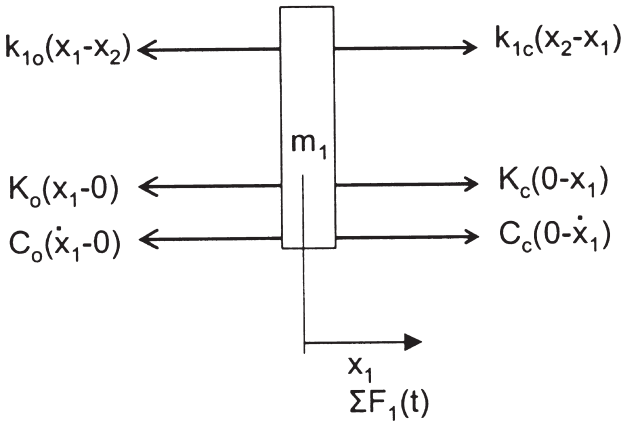

Figure 4—Free-body diagram of m_1

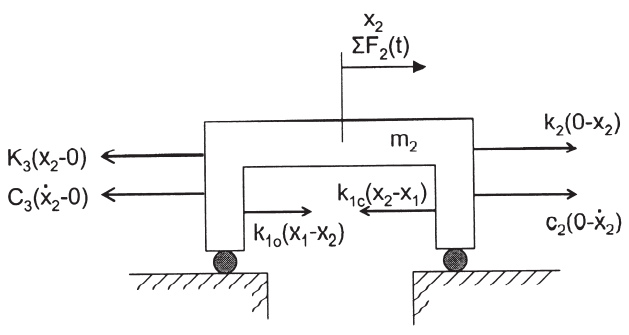

Figure 5—Free-body diagram of m_2

External forces

This section is concerned with the various external forces acting on m_1 and m_2. These are:

Fa_1: force on poppet due to incoming air
Fa_2: force on flip-flop from pressure inside the actuator
Fa_3: force on diaphragm from pressure inside actuator
F_w: load on plunger due to pressure build-up
F_0: force due to prestressing of main diaphragm spring
F_n: friction on plunger from seals.

The external force $\sum F_1(t)$ can be written as:

$$\sum F_1(t) = Fa_1(t) - Fa_2(t) \quad [8]$$

The flip-flop was assumed to move frictionlessly. Similarly, the external force $\sum F_2(t)$ can be written as:

$$\sum F_2(t) = Fa_3(t) - Fn - Fw - F_o \quad [9]$$

The sign of Fn will depend on the direction of the plunger displacement.

Force on poppet—Fa_1

The force on the poppet as a result of the incoming air is a function of the position of the poppet itself. When the poppet is closed, the resulting force on the poppet can be determined balancing the forces acting on it:

$$Fa_1 = P_a A_{poppet} - P_{ch}(t) A_{popseal} \quad [10]$$

where:

P_a = the incoming air pressure [Pa]
$P_{ch}(t)$ = the pressure inside the actuator chamber [Pa]
A_{poppet} = is the surface area of the poppet head [m^2]
$A_{popseal}$ = the area of the hole inside the poppet valve seal [m^2]

Force on flip-flop—Fa_2

The force exerted on the flip-flop as a result of the pressure inside the actuator is a function of the position of the flip-flop. When the flip-flop is closed, the following relationship holds:

$$Fa_2 = 3 \times A_{ff}\left(P_{ch}(t) - atm\right) \quad [11]$$

where A_{ff} is the area of the exhaust holes (of which there are three), and atm represents atmospheric pressure.

Force on diaphragm—Fa_3

The force exerted on the diaphragm is a function of the pressure inside the actuator P(t) and the effective diameter of the actuator D_{eff}. As a result, the following relationship holds:

$$Fa_3 = P_{ch}(t)\frac{\pi}{4} D_{eff}^2 \quad [12]$$

Load on plunger—Fw

The load on the plunger can be calculated with:

$$Fw = P_w \times A_p \quad [13]$$

where P_w is the pressure due to a load on the AP, and A_p is the surface area of a cross-section of the plunger. This force can be treated either as constant or as fluctuating. For the purpose of the model, this force was held constant.

Force due to prestressing of main spring—F_0

During assembly of the AP, the main diaphragm spring is compressed, resulting in a constant force F_0 on the actuator plate. This force can be calculated with:

$$F_o = z \times k_2 \quad [14$$

where z is the distance by which the spring is pre-compressed during assembly and k_2 is the spring constant.

Friction on plunger—Fn

The friction on the plunger is very difficult to estimate theoretically or experimentally. It was decided to implement the relationship:

$$F_n = 0.02 \times Fw \quad [15]$$

which basically assumes that the friction on the plunger is 2% of the load on the AP.

Fluid mechanics aspects

The pressure in the actuator chamber drives the AP. The air flow into and out of the actuator chamber must therefore be known to model the AP's dynamics. This section describes the empirical models used to estimate the air flow. Figure 6 illustrates the relevant components in their positions when air enters the actuator chamber.

Simplifying approximations

The air flow is compressible, three-dimensional and unsteady, but to model the flow in such detail is impractical in the simulation model. The approximations used to retain only the dominant flow physics are discussed in this section.

Firstly, the flow is modelled as quasi-steady flow. This implies that the flow 'instantaneously' adjusts to changes in geometry, while the accumulation of air mass in the flow path (except for the actuator chamber) is not significant. This approximation is reasonable since the mechanical parts' movements are much slower than the speed of sound. Secondly, the transition from inflow to outflow is modelled to

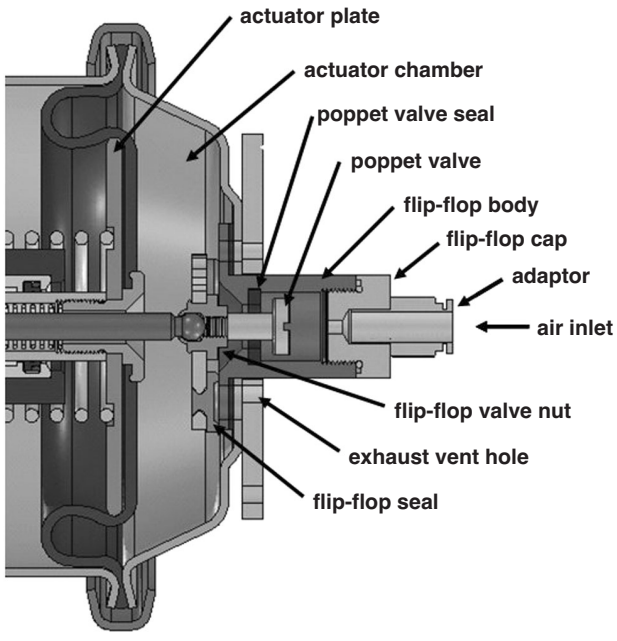

Figure 6—Components affecting air flow

occur instantaneously. This is reasonable since the period that the flip-flop moves from the one position to the other is small compared to the total cycle time of the AP. These two approximations make it possible to compute the mass flow of air entering or leaving the actuator chamber without knowing the details of the mechanism's movements at every instant. The flow rates can be calculated using only the air inlet pressure, instantaneous actuator chamber pressure, ambient pressure and flip-flop position (inlet open or closed).

Furthermore, the flow is modelled as one-dimensional flow, i.e. only variations in the main flow direction are modelled and empirical correlations are used where multi-dimensional flow effects are significant, e.g. when the flow area changes rapidly. The availability of appropriate empirical correlations limits the applicability of the model to sudden contractions and sudden expansions. Since the available correlations for 'minor losses' where derived for incompressible (low Mach number) flow, an adaptation to compressible flow had to be made, as discussed later.

The flow is modelled as adiabatic, i.e. heat exchange between the air and the flow channel is neglected, except that the actuator chamber is considered to be isothermal. The isothermal approximation simplifies the time integration, and numerical experiments showed that the errors incurred by this approximation are small enough for the cases considered here. The actuator chamber is further modelled as a plenum, i.e. complete mixing of the air occurs and velocities in the chamber are negligible. Air is modelled as a perfect gas, i.e. changes in the specific heat ratio (γ) are neglected, which induces very little error in the temperature ranges encountered.

The pressure at the air inlet is calculated as if the air comes from a large plenum, at the constant supply pressure, along a long, constant diameter hose in which pressure losses and heating due to friction are taken into account. The actual air supply in a mining situation was not available, but the approximation will capture the dominant effects of most practical situations. In the experimental work the air passed through a pressure regulator and through a supply hose, which is similar to the modelled situation.

Due to the large inlet pressures and typical AP geometries, choked flow (Mach=1) is encountered by the inflow just after the air inlet for most of the inflow part of the cycle. The flow path downstream of this point then has no influence on the mass flow rate and downstream frictional effects are therefore neglected. This approximation limits the model to air supply pressures of about 0.3 MPa or more.

Governing equations

The nomenclature used for the air flow model is as follows:

- A flow area [m^2]
- D_H hydraulic diameter [m]
- e wall roughness [m]
- m mass flow [kg/s]
- f D'Arcy friction factor
- K_c sudden contraction loss coefficient
- K_e sudden expansion loss coefficient
- M Mach number
- m_c mass of air in actuator chamber [kg]
- P stagnation pressure [Pa]
- p static pressure [Pa]
- R gas constant for air [287 kJ/(kg.K)]
- R_e Reynolds number
- T stagnation temperature [K]
- t static temperature [K]
- V flow velocity [m/s]
- V_c volume of actuator chamber [m^3]
- ρ density [kg.m^{-3}]
- γ specific heat ratio [J/(kg.K)]

subscripts

- 1 before
- 2 after

For the time integration procedure (see later) the instantaneous pressure differences (supply-to-plenum and plenum-to-ambient) are known and the inflow (flip-flop closed) or outflow (flip-flop open) mass flow rate is required. Since the computation of the mass flow rate as a function of pressure drop requires iteration (which would slow the time integration calculations down), the approach taken was to compute a number of combinations of mass flow vs. pressure drop, for inflow and outflow respectively, for each supply pressure that the simulation model was applied to. The time integration part then interpolated between the computed values.

The maximum inflow rate is limited to the choked mass flow (i.e. Mach=1 somewhere in the flow path) for the selected supply pressure. The critical actuator chamber pressure, i.e. the maximum pressure at which choked flow occurs, was determined by iteration. The choked mass flow was used when the chamber pressure was lower than the critical value. Flow rates at higher chamber pressures, with mass flows less than the critical, were then computed. For the outflow, there is no single choked mass flow rate, since the actuator chamber pressure varies continuously. The outflow rates were therefore computed for a range of chamber pressures varying between the supply pressure and ambient pressure, and the mass flow was restricted to the choked flow in each case where the pressure ratio exceeded the critical value.

Since adiabatic flow was assumed (i.e. T_0 remains constant) and the computation is done for a selected mass flow, only the change in P_0 over flow features had to be calculated to completely determine the thermodynamic state of the air at any given point. In one-dimensional flow, P_0 losses occur over sudden contractions, sudden expansion and in channels where friction is significant. Elbows in the flow path are usually modelled as equivalent lengths of flow channels with friction, but in typical APs, pressure losses associated with elbows are insignificant.

In incompressible flow, the pressure drop over a sudden contraction is given by the following Equation4:

$$p_1 - p_2 = \tfrac{1}{2} K_c \rho V_2^2 \qquad [16]$$

Two approaches were considered to convert this equation to compressible flow: in the first approach, the stagnation pressure ratio in compressible flow is assumed to be equivalent to the static pressure ratio in incompressible flow. This approach, however, gave convergence problems when seeking the choked mass flow. An alternative approach was therefore formulated: the stagnation pressure loss is proportional to the dynamic pressure (P–p), which agrees with the incompressible equation, and gives the following for compressible flow:

$$P_1 - P_2 = K_c\left(P_2 - p_2\right) \quad [17]$$

This equation gave stable, realistic results at all Mach numbers. The equation has to be solved iteratively since the pressure drop is a function of the outlet conditions. A similar approach is applied to the pressure drop over a sudden expansion, giving the following equation:

$$P_1 - P_2 = K_e\left(P_1 - p_1\right) \quad [18]$$

Fox and McDonald[4] give a graph of K_c and K_e vs. the area ratio of the contraction or expansion. A curve fit through a selection of points on this graph was used in the flow calculation.

To model the pressure losses associated with friction, the Fanno flow approximation, i.e. one-dimensional adiabatic flow with friction[5], was used. The frictional static pressure losses are given by the same equation as for incompressible flow since the friction coefficient is practically independent of the Mach number[5]. However, density changes require that the pressure loss be computed over short lengths only, giving:

$$dp_f = \tfrac{1}{2}\rho V^2 f\frac{dx}{D_H} \quad [19]$$

From the conservation of momentum then follows[5]:

$$dp + \rho V dV + \tfrac{1}{2}\rho V^2 f\frac{dx}{D_H} = 0 \quad [20]$$

This equation must be integrated numerically along the flow channel. Note that the second term cannot be neglected in compressible flows, particularly when approaching sonic velocities. Colebrook's friction factor formula and Miller's initial estimate were used[4]:

$$f^{-0.5} = -2\log_{10}\left[\frac{e}{3.7D_H} + \frac{2.51}{R_e f_0^{0.5}}\right] \quad [21a]$$

$$f_o = 0.25\left\{\log_{10}\left[\frac{e}{3.7D_H} + \frac{5.74}{R_e^{0.9}}\right]^{-2}\right\} \quad [21b]$$

The remaining equations required for computing the pressure drops are basic equations for compressible flow:

$$V = M\left(\gamma RT\right)^{0.5} \quad [22]$$

$$T = t\left[1 + \tfrac{1}{2}\left(\gamma - 1\right)M^2\right] \quad [23]$$

$$P = p\left(\frac{T}{t}\right)^{\frac{\gamma}{\gamma - 1}} \quad [24]$$

$$p = \rho R t \quad [25]$$

$$\dot{m} = \rho A V \quad [26]$$

Actuator chamber pressure

The pressure inside the actuator is determined by integrating the air mass flow rate into the chamber, thus giving the instantaneous mass of air in the chamber (m_c), the perfect gas law (Equation [25]) and $\rho = m_c/V_c$. For the results presented below, the temperature t was taken to be 25°C.

The volume of the actuator chamber varies as the actuator plate moves. The flexible diaphragm allows the movement, but complicates the calculation of the exact volume of the actuator chamber. To estimate the volume of the actuator chamber, it is approximated to be a function of the position of the actuator plate (x_2), a 'dead' volume V_o and the physical size of the actuator. The dead volume V_o is the volume of the chamber with the actuator plate in the uttermost back position. The value for V_o was estimated from the solid CAD model of the AP. The actual volume is then determined with:

$$V_c = \left(\frac{\pi}{4}d_{eff}^2\right)x_2 + V_o \quad [27]$$

where d_{eff} represents an effective volumetric diameter of the diaphragm. The exact value for d_{eff} also depends on the position of the actuator plate inside the chamber. The following equation was used to estimate d_{eff}:

$$d_{eff} = d_{c1} + \frac{x_2}{L_v}d_{c2} \quad \text{if } x_2 < L_v \quad [28a]$$

$$d_{eff} = d_{c2} \quad \text{if } x_2 \geq L_v \quad [28b]$$

where:

d_{c1} = minimum diameter of actuator [mm]
d_{c2} = maximum diameter of actuator [mm]
L_v = length of tapered part of actuator [mm]

Mass of air in chamber

Equations [17] to [26] provided a relationship between the mass flow rate, the inlet air pressure, the pressure in the chamber, and the direction of the air flow, i.e.:

$$\dot{m} = f\left(P_a, P_{ch}, fflop\right) \quad [29]$$

where:

$\dot{m}$ = mass flow rate of the air [kg/s]
P_a = the inlet air pressure [bar]
P_{ch} = the pressure inside the chamber [bar]
fflop = indicates if the flip-flop valve is open or closed [0 or 1]

This relationship was provided in the form of a 'look-up table' for each inlet air pressure P_a, which yields the mass flow rate as a function of the pressure in the chamber P_{ch}. The mass of air inside the chamber is then determined through numerical integration of Equation [29]. From this, Equations [25] and [27] are used to solve the pressure inside the chamber for each position of x_2.

Time integration

The equations from the previous sections were programmed in MATLAB for numerical simulation. The program essentially consists of a main body where all the input data must be entered. The main body employs a subroutine that can numerically integrate any given function. In this case, the integration function is Equation [7], together with integration of the mass flow rate from Equation [29]. The main program is supplied with a total time span for simulation, and hence the total span is divided into many small steps. The main program is also supplied with initial values for the unknowns, which serves as a starting point for the simulation.

During the integration process, the pressure inside the actuator and the external forces are calculated for each time instant. The pressure and forces are functions of the unknowns, x_1 and x_2, and as a result the previous step's values for x_1 and x_2 are used to calculate the pressure and forces.

Since the equations for the air flow are coupled and non-linear, iterations were used to compute the stagnation pressure at each significant point along the flow path. The program's algorithm uses estimates of the inlet mass flow to compute the complete flow path, and therefore the associated chamber pressure. For the outflow, the mass flow was iteratively determined for a selected chamber pressure. The variation of loss coefficients (contraction and expansion) with area ratio, given by Fox and McDonald[4] was used in the program.

Experimental set-up

The 'New Concept Mining Air Pump Test Station' at Stellenbosch University was used for experiments to validate the model. A photo of the test bench with the mounted AP is shown in Figure 7.

A diagram of the test station is shown in Figure 8. Two rotameters were installed to measure the air and water flow rates. The air inlet pressure is regulated with a pressure regulator. The load (or back pressure) on the AP is controlled by means of a needle valve at the water outlet. The load on the AP simulates the physical conditions when the AP is inflating a mining prop or roof bolt. Analogue pressure gauges are installed on each line. The AP is rigidly mounted on the base plate on top of the table.

The displacements of the diaphragm and flip-flop were measured with laser displacement sensors. The water and air pressures were collected with voltage-type pressure transducers. The exact measurement points for the laser sensors can be observed in Figure 9, and the pressure transducers are visible in Figure 7. The displacement transducers are clamped on brackets mounted on the table. The pressure transducers are directly mounted on the AP, one on the actuator air side, and the other at the water outlet.

A four-channel Spectral Dynamics Siglab[6] was used to collect data. A description of the measurement parameters is shown in Table I, and a list of the measurement equipment is shown in Table II. The water inlet pressure was kept at 3.5 bar during all the tests. The set-up of the sensors and the measurement equipment is diagrammatically depicted in Figure 10.

Results

Several simulations were conducted to ensure that the model performed adequately at different load and air inlet conditions. It should be noted that the model does not perform very well at low air inlet pressures. At low air inlet pressures, the model is extremely sensitive to the AP's geometry, and the pressure drop for air entering the chamber might be higher than the model predicts. Further refinement of the air flow model would be required if a more accurate description of the AP's behaviour is required at low air inlet pressures. The following figures (Figure 11–Figure 14) are a selection of simulations comparing the model performance with the experimental data.

Discussion

From the above figures it can be observed that the model corresponds fairly well with the experimental data. Slight differences in the speeds of pumping (i.e. frequency of reciprocation) can be observed, and this can be attributed to:

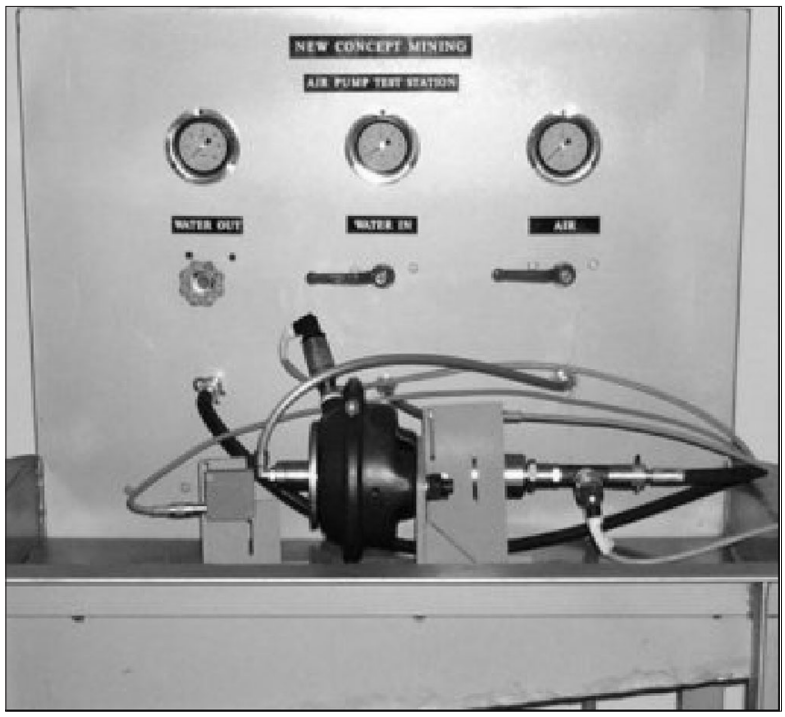

Figure 7—New Concept Mining Air Pump Test Station

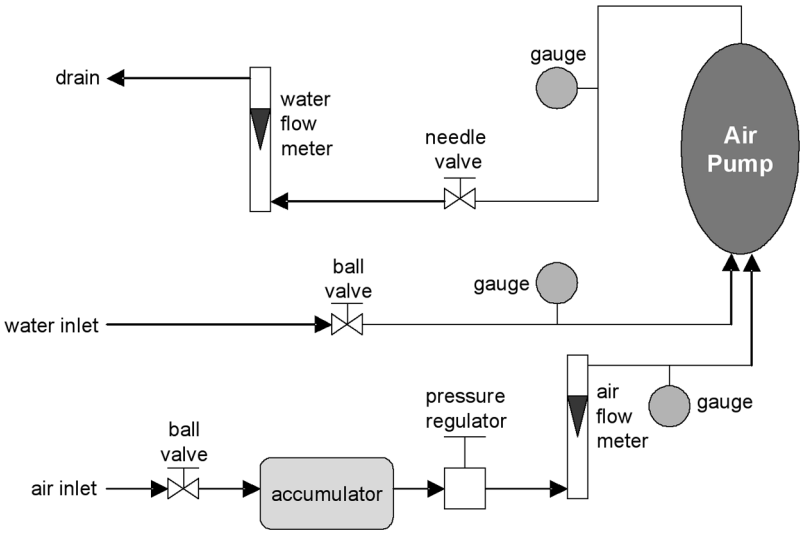

Figure 8—NCM Test Station diagrammatic layout

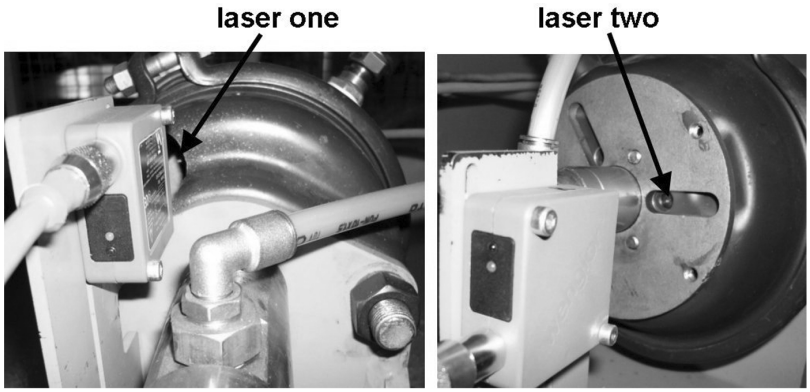

Figure 9—Position of lasers

Table I

Measurement parameters

Parameter	Value
Frequency range	1000 Hz
Record length	8192 samples
Period	3.2 seconds
Window	off
Sampling frequency (each channel)	2560 Hz

Table II

Measurement equipment

Type	Model	Sensitivity
Laser 50–100 mm	WENGLOR YP11MGV80	20 mV/mm
Laser 50–100 mm	WENGLOR YP11MGVL80S540	20 mV/mm
Pressure 6 bar	RS 249-3959	16.67 mV/bar
Pressure 40 MPa	RS 348-8217	2.5 mV/MPa
Analyser	Siglab 20-42	16-bit

- imperfections in setting up an exact load on the AP during the experiments
- assumptions in the model, e.g. nonlinearity of springs and damping effects
- in the model there is a constant load on the plunger, but in reality the load on the plunger fluctuates

It was also clear that the model becomes less accurate at extreme loads on the AP and also in the low air inlet pressure range. The computed pressure in the chamber does not always drop as low as the experimentally measured pressure, and this is also attributed to the load on the plunger that remains constant in the model whereas it fluctuates in reality.

Conclusion

A parametric analytical model that models the behaviour of the New Concept Mining Air Pump was presented in this paper. Very good correlation between the model performance and measured data was found. Slight discrepancies between the model and the measured experimental data are a result of fluctuating loads on the AP, as well as other assumptions in the model. The model is also less accurate at extreme loads on the AP and in the low air inlet pressure range. A more

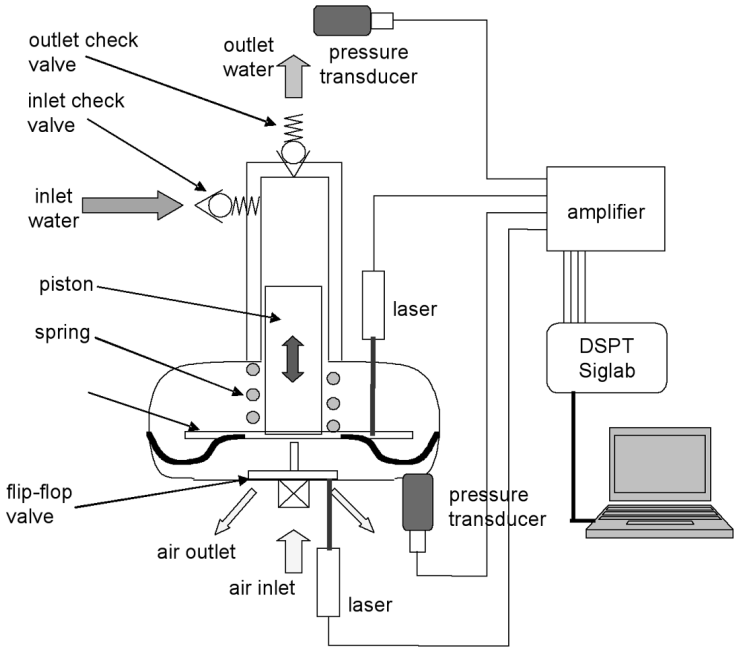

Figure 10—Diagram of AP and sensors

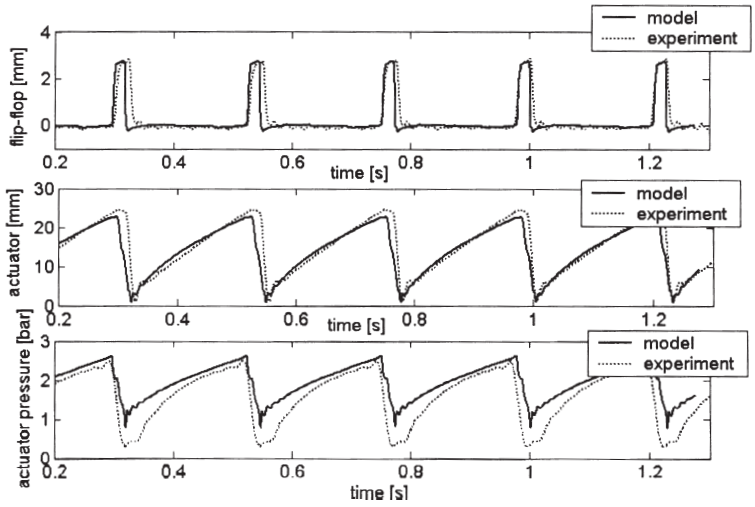

Figure 11—Model performance, 3 bar air inlet with 4 MPa load

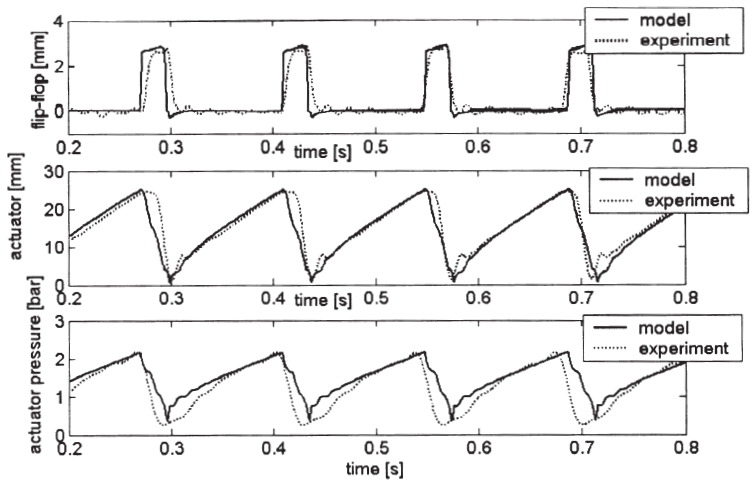

Figure 12—Model performance, 4 bar air inlet with 2 MPa load

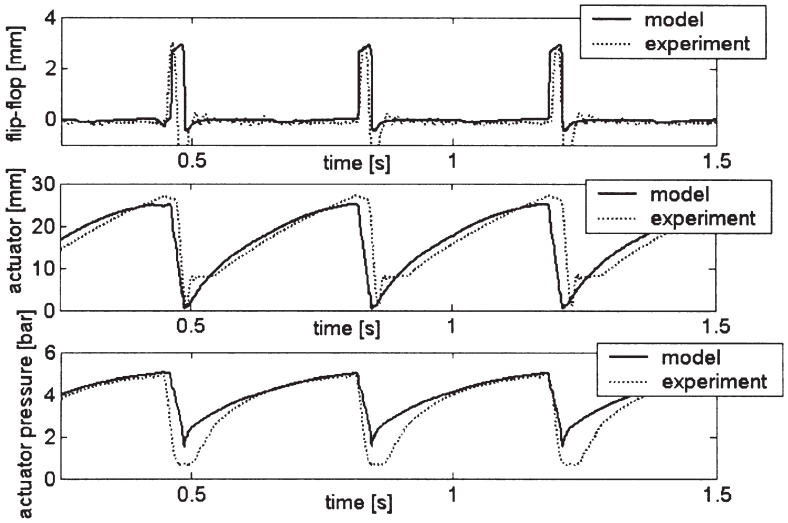

Figure 13—Model performance, 5 bar air inlet with 11 MPa load

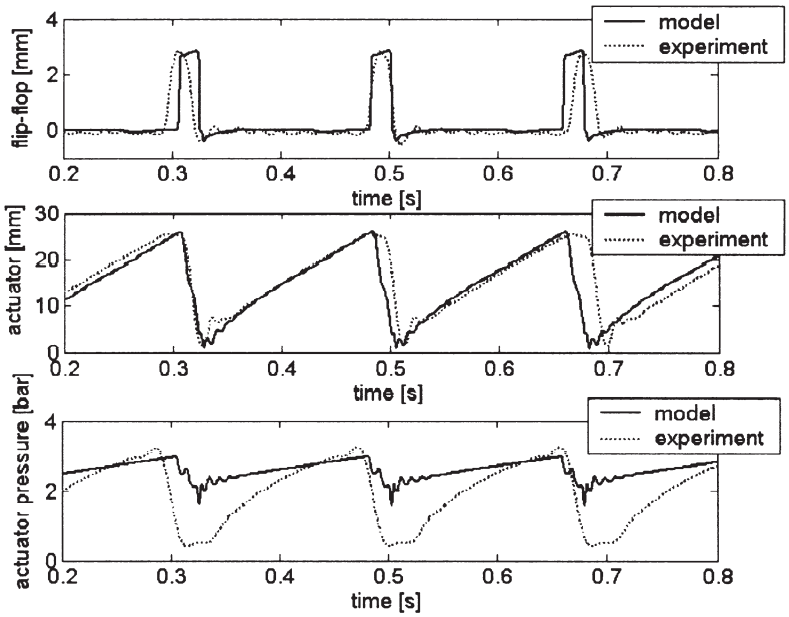

Figure 14—Model performance, 6 bar air inlet with 7 MPa load

accurate estimation at these conditions will require refinement of the model or possibly a computational fluid dynamics (CFD) analysis.

It was discovered that the air flow into the AP is controlled by the small opening in the flip-flop cap. The optimal diameter of this opening was determined through model simulations and a recommendation was made for future designs. Furthermore, it was found that the flow of air out of the AP is controlled by the exhaust hole diameters. The performance of the AP as a function of the exhaust hole diameters was investigated and optimal values for future designs were recommended. The design variables of the three springs that are responsible for controlling the actions of the diaphragm and flip-flop were also optimized to improve the AP's reliability and improve its performance over a wider range of operating conditions. Using the model simulations, an updated design was recommended that should yield an overall improvement of about 80% in flow rate and a 30% increase in the pressure that can be delivered. This will ensure that the AP can be used safely to inflate mining props even when the air supply pressure is low.

Acknowledgements

The financial and material support of New Concept Mining is gratefully acknowledged.

REFERENCES

1. Rao, S.S. *Mechanical Vibrations*, 3rd edition, Addison-Wesley, 1995.
2. MATLAB by Mathworks, http://www.mathworks.com
3. Mathews, J.H. *Numerical Methods for Mathematics, Science and Engineering*, 2nd edition, Prentice-Hall, 1992.
4. Fox, R.W. and MacDonald, A.T. *Introduction to Fluid Mechanics*, 3rd edition, John Wiley & Sons, 1985.
5. Zucrow, M.J. and Hoffman, J.D. Gas Dynamics, Vol. 1, John Wiley & Sons, 1976.
6. Spectral Dynamic Siglab, http://www.spectraldynamics.com ◆